

Electronic Supplementary Information (ESI)

Rigid versions of PDTA⁴⁻ incorporating a 1,3-diaminocyclobutyl spacer for Mn²⁺ complexation: stability, water exchange dynamics and relaxivity

Rocío Uzal-Varela,^a Daniela Lalli,^b Isabel Brandariz,^a Aurora Rodríguez-Rodríguez,^{*,a}
Carlos Platas-Iglesias,^a Mauro Botta,^b and David Esteban-Gómez^a

^a Universidade da Coruña, Centro de Investigacións Científicas Avanzadas (CICA) and Departamento de
Química Fundamental, Facultade de Ciencias, 15071, A Coruña, Galicia, Spain.

^b Magnetic Resonance Platform (PRISMA-UPO), Dipartimento di Scienze e Innovazione Tecnologica,
Università del Piemonte Orientale “A. Avogadro”, Viale T. Michel 11, 15121 Alessandria, Italy.

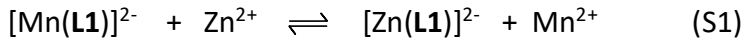
Summary

Dissociation kinetics	4
Figure S1. Absorption spectra of the $[\text{Mn}(\text{L1})]^{2-}$ - Zn^{2+} reacting system before (bold trend) and 5 min after (red trend) the mixing of the reactant ($[\text{MnL}] = 0.25 \text{ mM}$, $[\text{Zn}^{2+}] = 1.25 \text{ mM}$, $[\text{HEPES}] = 0.01 \text{ M}$, $\text{pH} = 7.4$, $l = 0.874 \text{ cm}$, 0.15 M NaCl , 25°C).	7
Figure S2. Pseudo-first-order rate constant (k_d) characterising the transmetallation reaction between $[\text{Mn}(\text{L1})]^{2-}$ and Zn^{2+} ($[\text{MnL}]_t = 0.25 \text{ mM}$, $[\text{HEPES}] = 0.01 \text{ M}$, 0.15 M NaCl , 25°C)	7
Figure S3. Absorption spectra of the different protonated forms of the L2^{2-} ligand calculated from spectrophotometric titrations in aqueous solution (0.15 M NaCl , 25°C).	8
Figure S4. Absorption spectrum recorded from an equimolar mixture of L2^{2-} and Mn^{2+} ($9.11 \times 10^{-5} \text{ M}$, $\text{pH} = 4.75$, 0.15 M NaCl , 25°C , circles), fitted spectrum (green line) and spectral contributions of the different species present in solution.	9
Figure S5. Absorption spectral changes observed during the formation of the $[\text{Mn}(\text{L2})]$ complex in aqueous solution in the pH range 3.9-6.9 (0.15 M NaCl , 25°C).	10
Figure S6. Potentiometric titrations of the L1^{4-} ligand (3.92 mM) in the absence and in the presence of one equivalent of Mn^{2+} (0.15 M NaCl , 25°C).....	11
Figure S7. ^1H NMR spectrum of compound 1 (500 MHz, CDCl_3 , 298 K).....	12
Figure S8. ^{13}C NMR spectrum of compound 1 (101 MHz, CDCl_3 , 298 K).....	12
Figure S9. Experimental high resolution mass spectrum (ESI^+) of compound 1	13
Figure S10. ^1H NMR spectrum of $\text{H}_4\text{L1}$ (500 MHz, D_2O , $\text{pH} = 1.70$, 298 K).....	14
Figure S11. ^{13}C NMR spectrum of $\text{H}_4\text{L1}$ (126 MHz, D_2O , $\text{pH} = 1.70$, 298 K).....	14
Figure S12. Experimental high resolution mass spectrum (ESI^-) of $\text{H}_4\text{L1}$	15
Figure S13. ^1H NMR spectrum of $\text{H}_2\text{L3}$ (500 MHz, D_2O , $\text{pH} = 2.10$, 298 K).....	16
Figure S14. ^{13}C NMR spectrum of $\text{H}_2\text{L3}$ (126 MHz, D_2O , $\text{pH} = 2.10$, 298 K).....	16
Figure S15. ^1H NMR spectrum of $\text{H}_2\text{L3}$ (300 MHz, D_2O , $\text{pH} = 2.10$, 343 K).....	17
Figure S16. ^{13}C NMR spectrum of $\text{H}_2\text{L3}$ (75.5 MHz, D_2O , $\text{pH} = 2.10$, 343 K).....	17
Figure S17. Experimental high resolution mass spectrum (ESI^+) of $\text{H}_2\text{L3}$	18
Figure S18. ^1H NMR spectrum of compound 2 (300 MHz, CDCl_3 , 298 K).....	19
Figure S19. ^{13}C NMR spectrum of compound 2 (75.5 MHz, CDCl_3 , 298 K).....	19

Figure S20. Experimental high resolution mass spectrum (ESI^+) of compound 2	20
Figure S21. ^1H NMR spectrum of compound 3 (400 MHz, CDCl_3 , 298 K).....	21
Figure S22. ^{13}C NMR spectrum of compound 3 (101 MHz, CDCl_3 , 298 K).....	21
Figure S23. Experimental high resolution mass spectrum (ESI^+) of compound 3	22
Figure S24. ^1H NMR spectrum of H₂L2 (500 MHz, D_2O , pH 4.33, 298 K).....	23
Figure S25. ^{13}C NMR spectrum of H₂L2 (126 MHz, D_2O , pH 4.33, 298 K).....	23
Figure S26. Experimental high resolution mass spectrum (ESI^+) of H₂L2	24
Table S1. Optimized Cartesian coordinates obtained for $[\text{Mn}(\text{EDTA})(\text{H}_2\text{O})]^{2-}\cdot 5\text{H}_2\text{O}$ (M11/Def2-TZVPP, scrf=pcm).	25
Table S2. Optimized Cartesian coordinates obtained for $[\text{Mn}(\text{L1})(\text{H}_2\text{O})]^{2-}\cdot 5\text{H}_2\text{O}$ (M11/Def2-TZVPP, scrf=pcm).	27
Table S3. Optimized Cartesian coordinates obtained for $[\text{Mn}(\text{L2})(\text{H}_2\text{O})]\cdot 2\text{H}_2\text{O}$ (M11/Def2-TZVPP, scrf=pcm).	29
Table S4. Optimized Cartesian coordinates obtained for $[\text{Mn}(\text{L3})(\text{H}_2\text{O})]\cdot 2\text{H}_2\text{O}$ (M11/Def2-TZVPP, scrf=pcm).	31
References	33

Dissociation kinetics

The rates of the transmetallation reactions (Eq. (S1)) between $[\text{Mn}(\text{L1})]^{2-}$ and Zn^{2+} were studied by spectrophotometry. Some characteristic absorption spectra of the $[\text{Mn}(\text{L1})]^{2-} - \text{Zn}^{2+}$ system are shown in Figure S1.



According to the spectrophotometric studies of the transmetallation reaction between $[\text{Mn}(\text{L1})]^{2-}$ and Zn^{2+} (Figure S1), the replacement of the Mn^{2+} -ion with Zn^{2+} results in the decreases of the absorbance values at <235 nm. Based on the spectral changes, it might be assumed that the absorption band of the carboxylate groups of $[\text{Mn}(\text{L1})]^{2-}$ is shifted to the lower wavelength range by the formation of $[\text{Zn}(\text{L1})]^{2-}$ due to the stronger interaction between the $-\text{COO}^-$ and the Zn^{2+} ion compared to the Mn^{2+} ion. Moreover, the relatively short reaction timescale of the transmetallation process obtained from the spectrophotometric studies was also confirmed by the investigation of the $[\text{Mn}(\text{L1})]^{2-} - \text{Zn}^{2+}$ reacting system with T_1 measurements.

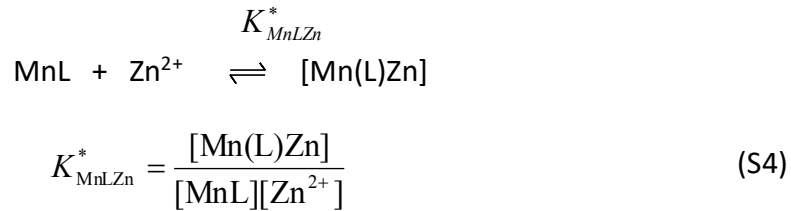
In the presence of excess of the exchanging ion, the transmetallation can be treated as a pseudo-first-order process and the reaction rate can be expressed with Eq. (S2), where k_d is a pseudo-first-order rate constant and $[\text{MnL}]_t$ is the total concentration of the Mn^{2+} -complex.

$$-\frac{d[\text{MnL}]_t}{dt} = k_d [\text{MnL}]_t \quad (\text{S2})$$

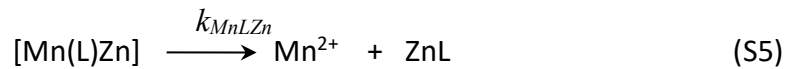
The rates of the transmetallation reactions were studied at different concentrations of the exchanging metal ion at pH=7.4. The obtained pseudo-first order rate constants k_d are presented in Figure S2 as a function of $[\text{Zn}^{2+}]$.

At pH = 7.4 the k_d values increase with $[\text{Zn}^{2+}]$. The dependence of k_d on the $[\text{Zn}^{2+}]$ can be expressed as a first-order function of $[\text{Zn}^{2+}]$ which indicates that the exchange can take place by Zn^{2+} -independent and Zn^{2+} -assisted dissociation pathways. The Zn^{2+} -independent pathway can be explained by the spontaneous dissociation of $[\text{Mn}(\text{L1})]^{2-}$ (k_0 , Eq. (S3)), which is followed by the rapid reaction of the free ligand with the exchanging Zn^{2+} ion. The Zn^{2+} assisted reaction can be interpreted by the direct attack

of the exchanging metal ion on the $[\text{Mn}(\text{L1})]^{2-}$ complex via the formation of dinuclear intermediate characterized by the K^*_{MnLZn} stability constant (Eq. (S4)). In the case of the $[\text{Mn}(\text{EDTA})]^{2-}$, $[\text{Mn}(\text{CDTA})]^{2-}$ and $[\text{Mn}(\text{PDTA})]^{2-}$ complexes the formation of the hetero-dinuclear complexes with Cu^{2+} was also detected by spectrophotometry.¹



It can be assumed that in the dinuclear intermediate Mn(L)Zn , the functional groups of the **L1**⁴⁻ ligand are slowly transferred from Mn^{2+} to the attacking Zn^{2+} ion (k_{MnLZn} , Eq. (S5)).



By taking into account all the possible pathways, the rate of the transmetallation of $[\text{Mn}(\text{L1})]^{2-}$ with Zn^{2+} can be expressed by Eq. (S6), where $[\text{MnL}]$ and $[\text{Mn(L)Zn}]$ are the concentrations of the free and dinuclear complexes, respectively:

$$-\frac{d[\text{MnL}]_t}{dt} = k_d[\text{MnL}]_t = k_0[\text{MnL}] + k_{\text{MnLZn}}[\text{Mn(L)Zn}] \quad (\text{S6})$$

Thus, the pseudo-first-order rate constant (k_d) can be expressed as in (Eq. (S7)) considering the total concentration of $[\text{Mn}(\text{L1})]^{2-}$ ($[\text{MnL}]_t = [\text{MnL}] + [\text{Mn(L)Zn}]$), the stability constant of the dinuclear $[\text{Mn(L)Zn}]$ intermediate (K^*_{MnLZn} , Eq. (S4)) and Eq. (S6)).

$$k_{obs} = \frac{k_0 + k_3^{Zn}[\text{Zn}^{2+}]}{1 + K^*_{\text{MnLZn}}[\text{Zn}^{2+}]} \quad (\text{S7})$$

The rate constants $k_1 = k_{\text{GdH2L}} \times K_{\text{GdHL}}^{\text{H}}$ and $k_3 = k_{\text{GdLCu}} \times K_{\text{GdLCu}}$ characterise the spontaneous and Zn^{2+} -assisted dissociation of $[\text{Mn}(\text{L1})]^{2-}$, respectively. The stability constant of dinuclear $[\text{Mn(L)Zn}]$ intermediates formed with the rigid ligand are relatively small (e.g. $[\text{Mn}(\text{CDTA})\text{Cu}]$: $K^*_{\text{MnLCu}}=79$).¹ By taking into account the very low stability constant of the $[\text{Mn(L1)Zn}]$ intermediate ($K^*_{\text{MnLCu}}<100$), the denominator of Eq. (S7) can be neglected ($1>>K^*_{\text{MnLZn}}[\text{Zn}^{2+}]$), so Eq. (S7) can be simplified in the form of Eq. (S8). The

k_0 and k_3^{Zn} values have been calculated by fitting of the kinetic data (Figure S2) to Eq. (S8).

$$k_{\text{obs}} = k_0 + k_3^{\text{Zn}} [\text{Zn}^{2+}] \quad (\text{S8})$$

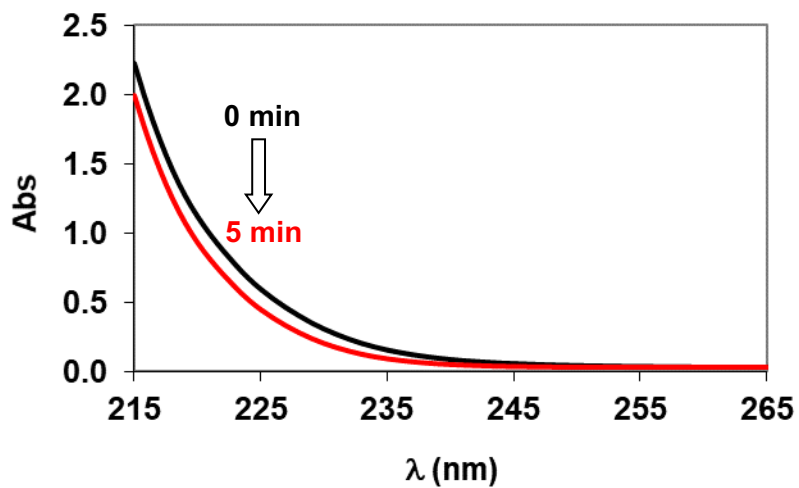


Figure S1. Absorption spectra of the $[\text{Mn}(\text{L1})]^{2-}$ - Zn^{2+} reacting system before (black trace) and 5 min after (red trace) the mixing of the reactant ($[\text{MnL}]_t=0.25$ mM, $[\text{Zn}^{2+}]_t=1.25$ mM, $[\text{HEPES}]_t=0.01$ M, $\text{pH}=7.4$, $l=0.874$ cm, 0.15 M NaCl, 25 °C).

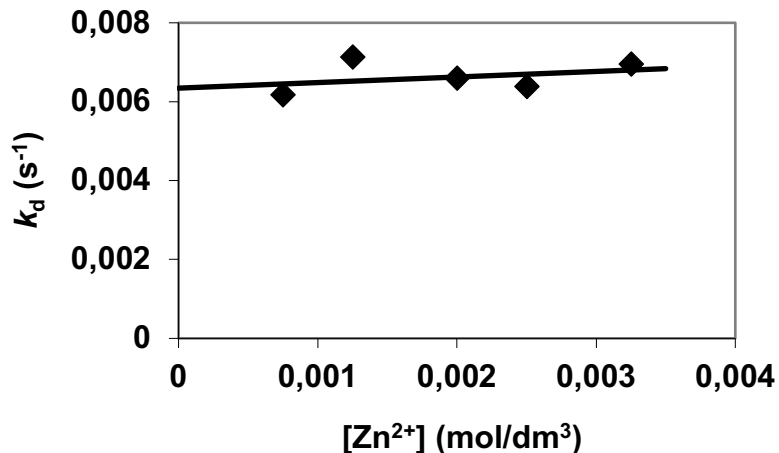


Figure S2. Pseudo-first-order rate constant (k_d) characterising the transmetallation reaction between $[\text{Mn}(\text{L1})]^{2-}$ and Zn^{2+} ($[\text{MnL}]_t=0.25$ mM, $[\text{HEPES}]_t=0.01$ M, 0.15 M NaCl, 25 °C).

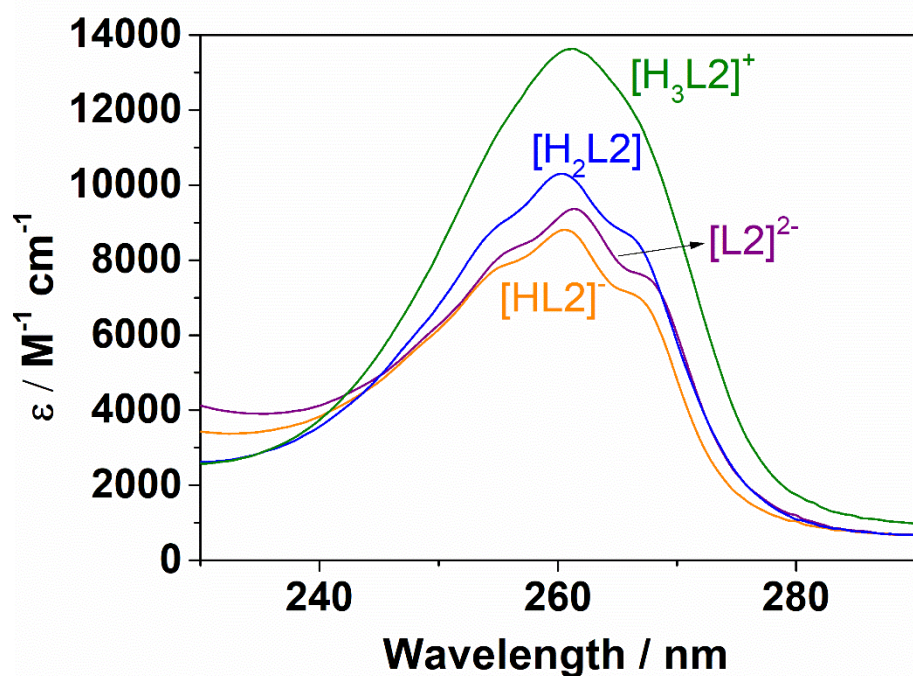


Figure S3. Absorption spectra of the different protonated forms of the L2^{2-} ligand calculated from spectrophotometric titrations in aqueous solution (0.15 M NaCl, 25°).

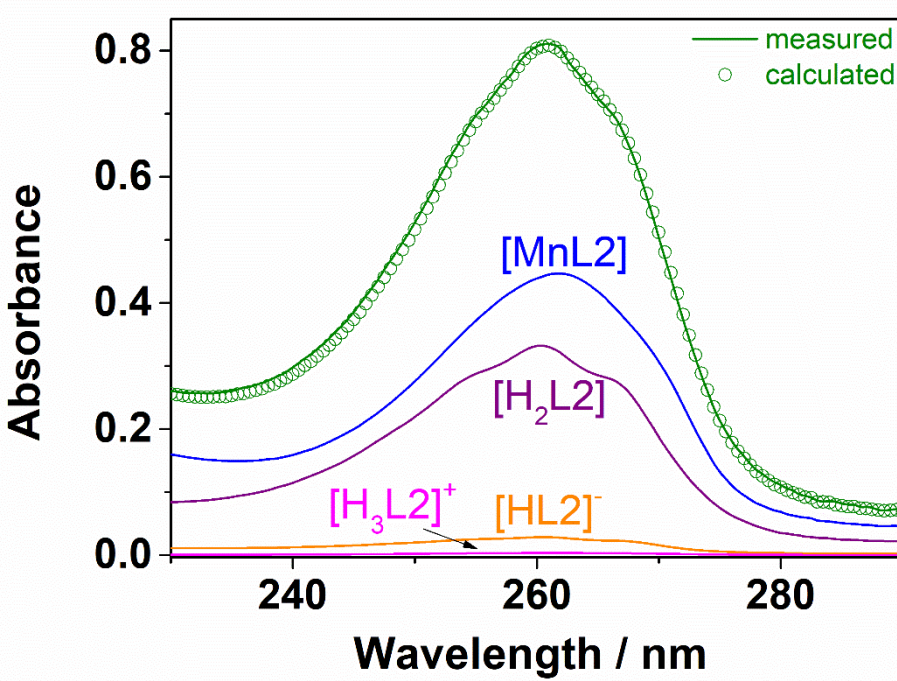


Figure S4. Absorption spectrum recorded from an equimolar mixture of $\text{L}2^{2-}$ and Mn^{2+} (9.11×10^{-5} M, pH 4.75, 0.15 M NaCl, 25°C, circles), fitted spectrum (green line) and spectral contributions of the different species present in solution.

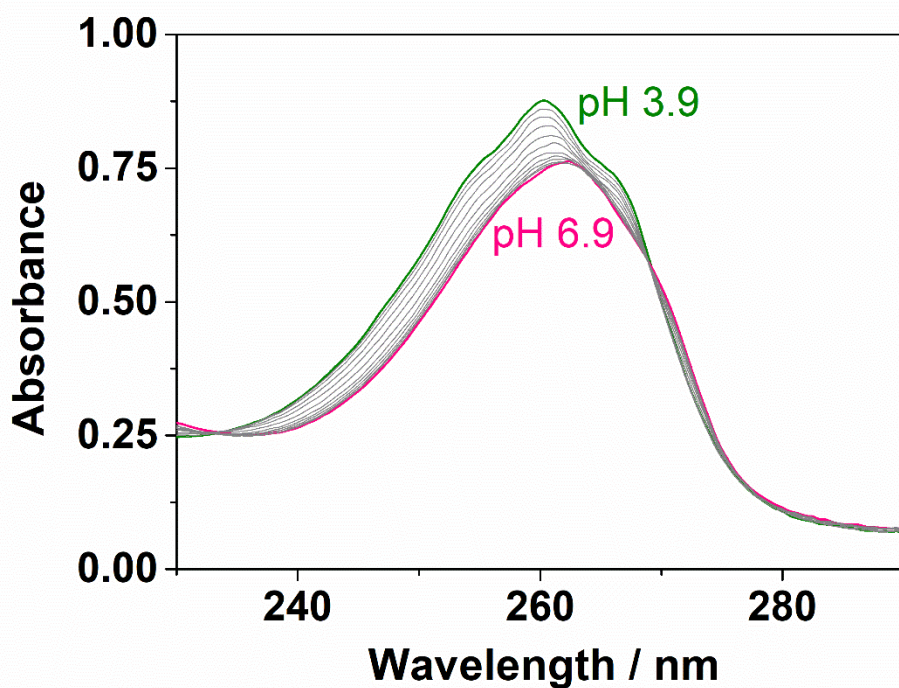


Figure S5. Absorption spectral changes observed during the formation of the $[\text{Mn}(\text{L2})]$ complex in aqueous solution in the pH range 3.9-6.9 (0.15 M NaCl, 25°C.).

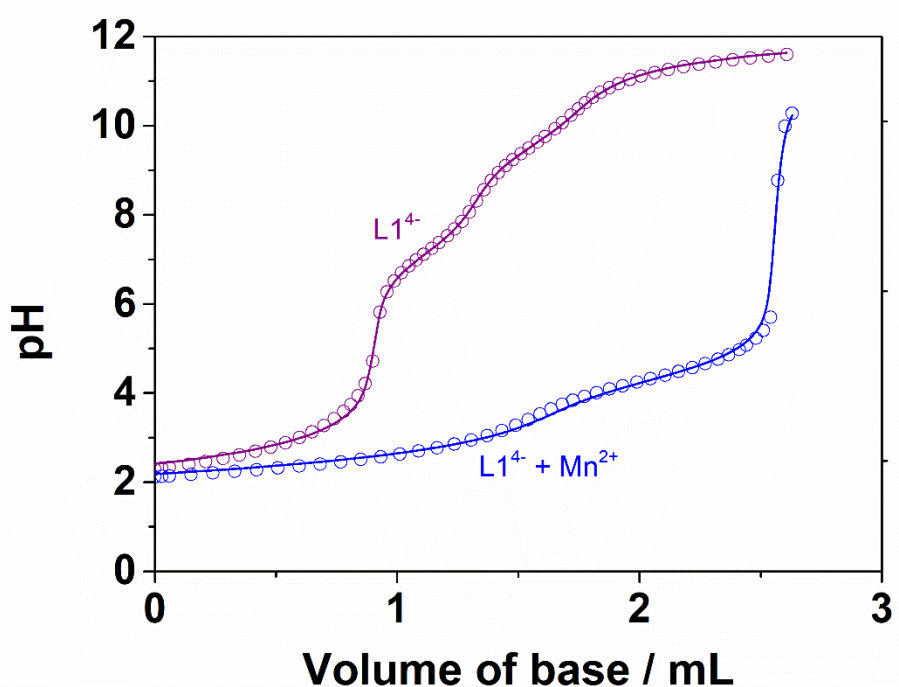


Figure S6. Potentiometric titrations of the L1^{4-} ligand (3.92 mM) in the absence and in the presence of one equivalent of Mn^{2+} (0.15 M NaCl, 25°C)

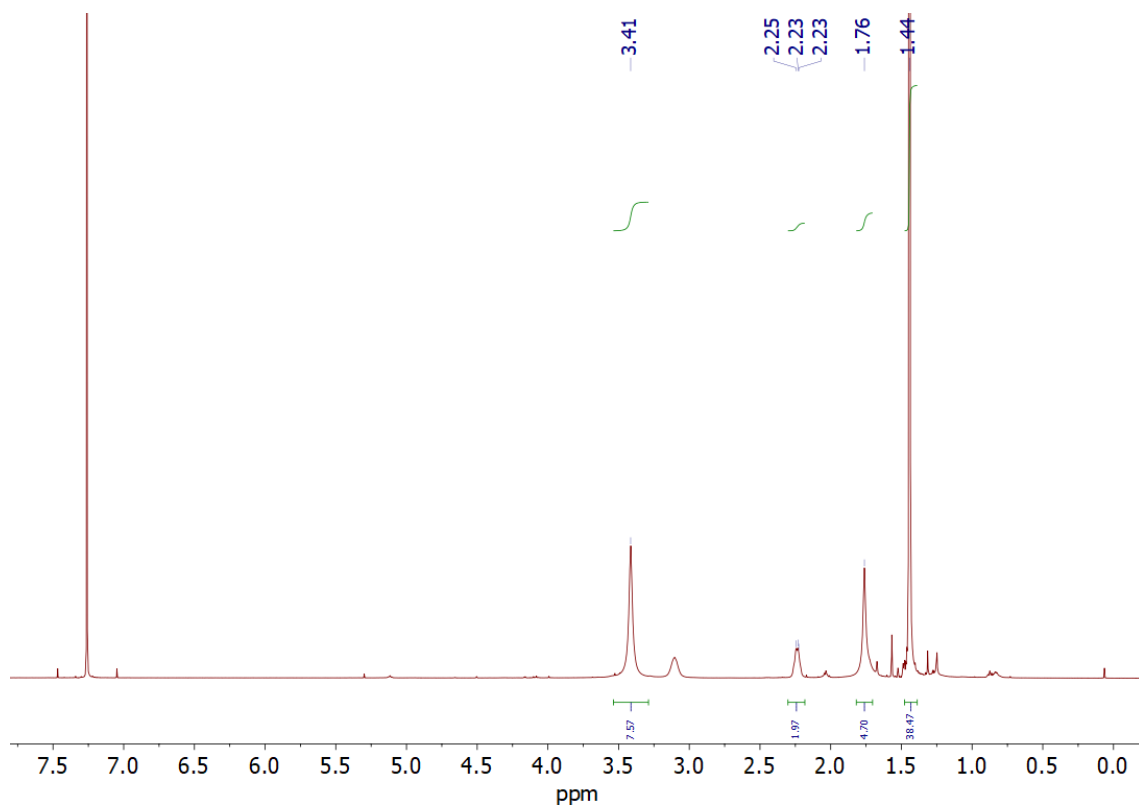


Figure S7. ¹H NMR spectrum of compound 1 (500 MHz, CDCl₃, 298 K).

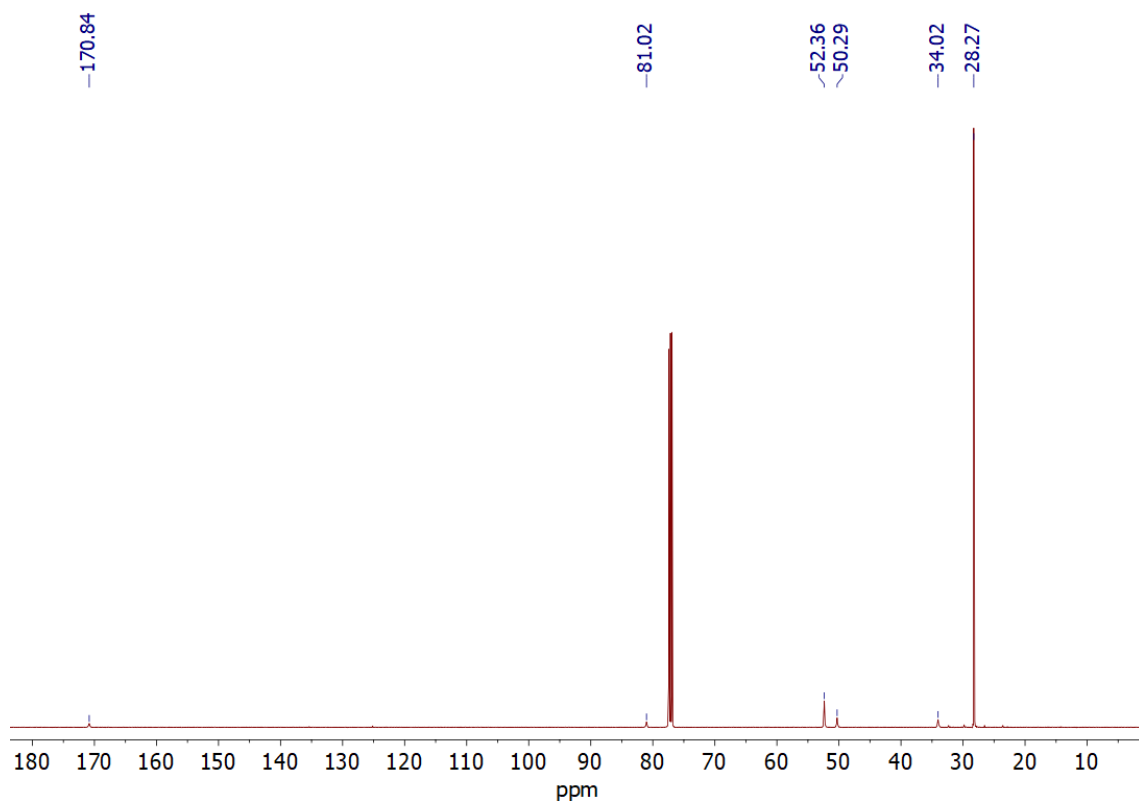


Figure S8. ¹³C NMR spectrum of compound 1 (101 MHz, CDCl₃, 298 K).

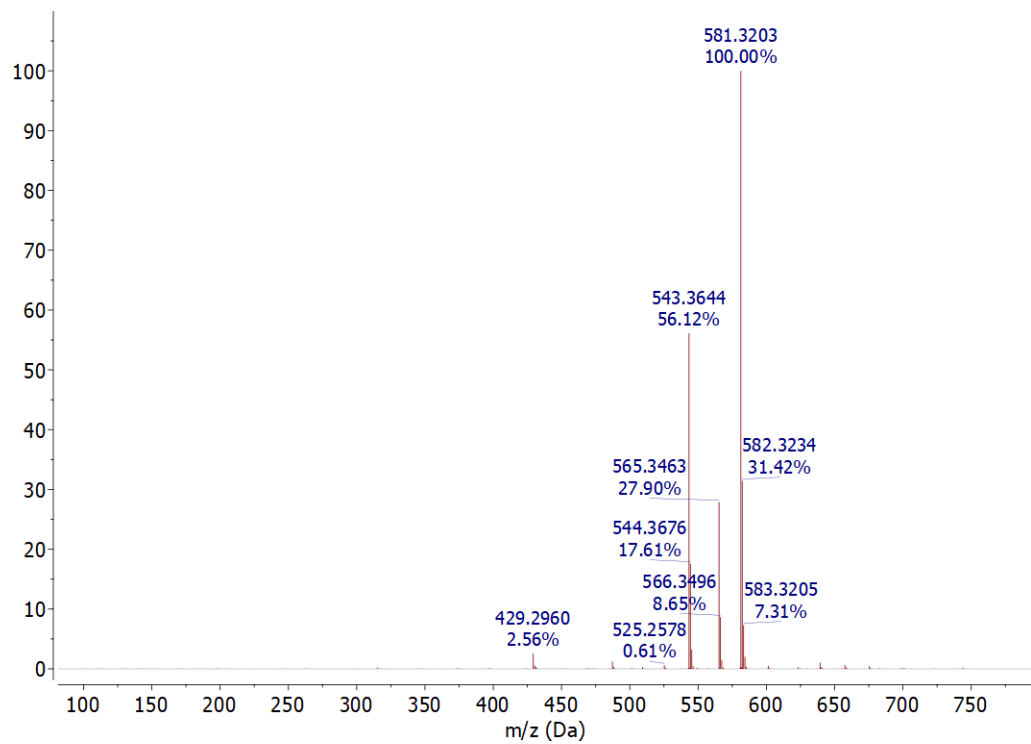


Figure S9. Experimental high resolution mass spectrum (ESI^+) of compound **1**.

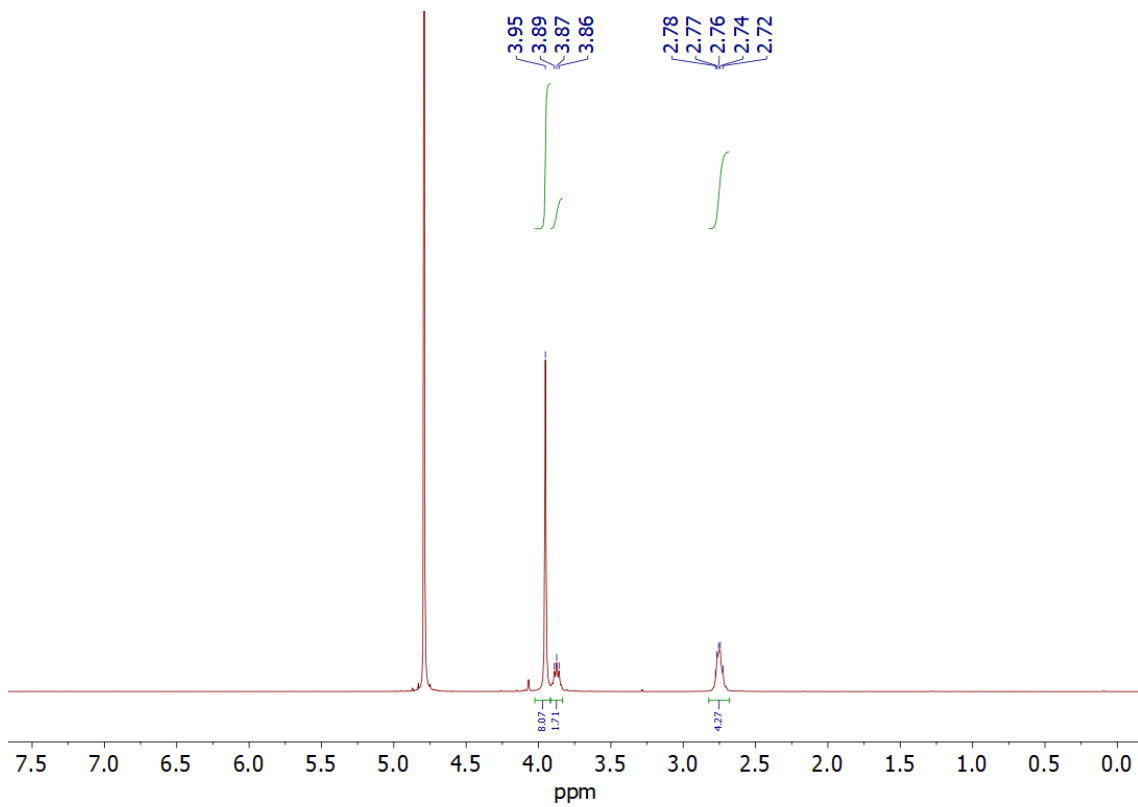


Figure S10. ¹H NMR spectrum of H₄L1 (500 MHz, D₂O, pH 1.70, 298 K).

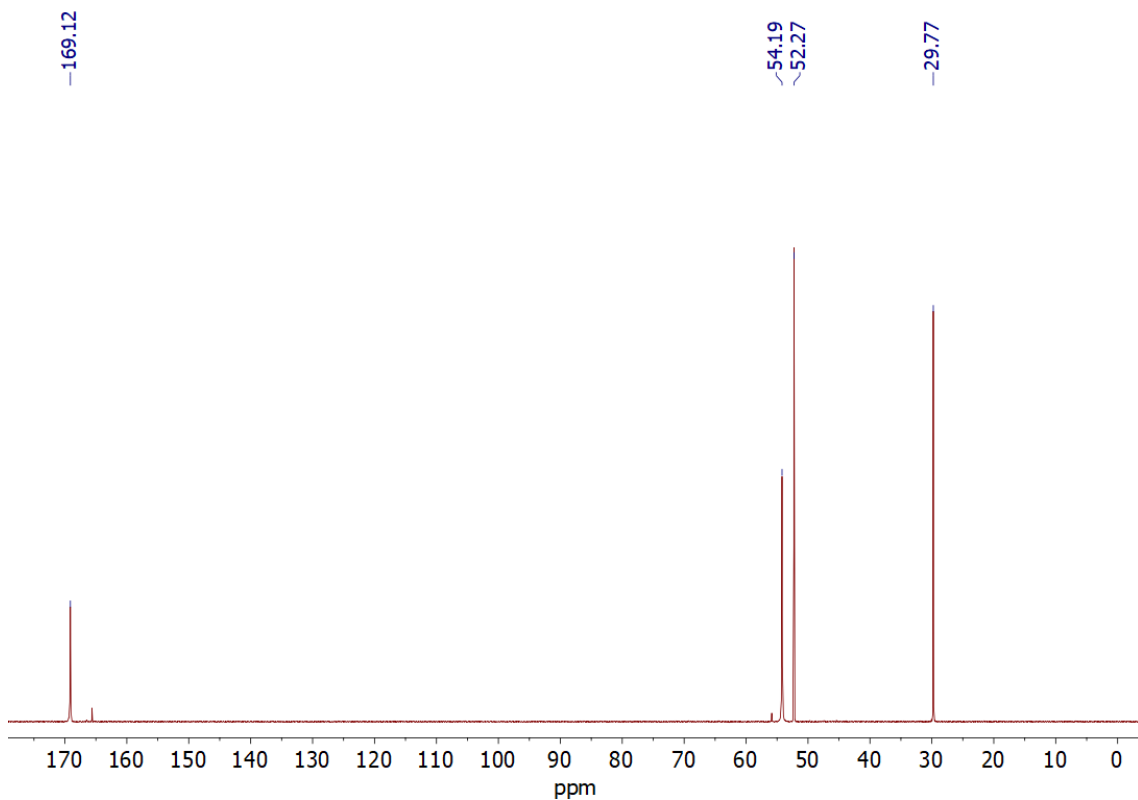


Figure S11. ¹³C NMR spectrum of H₄L1 (126 MHz, D₂O, pH 1.70, 298 K).

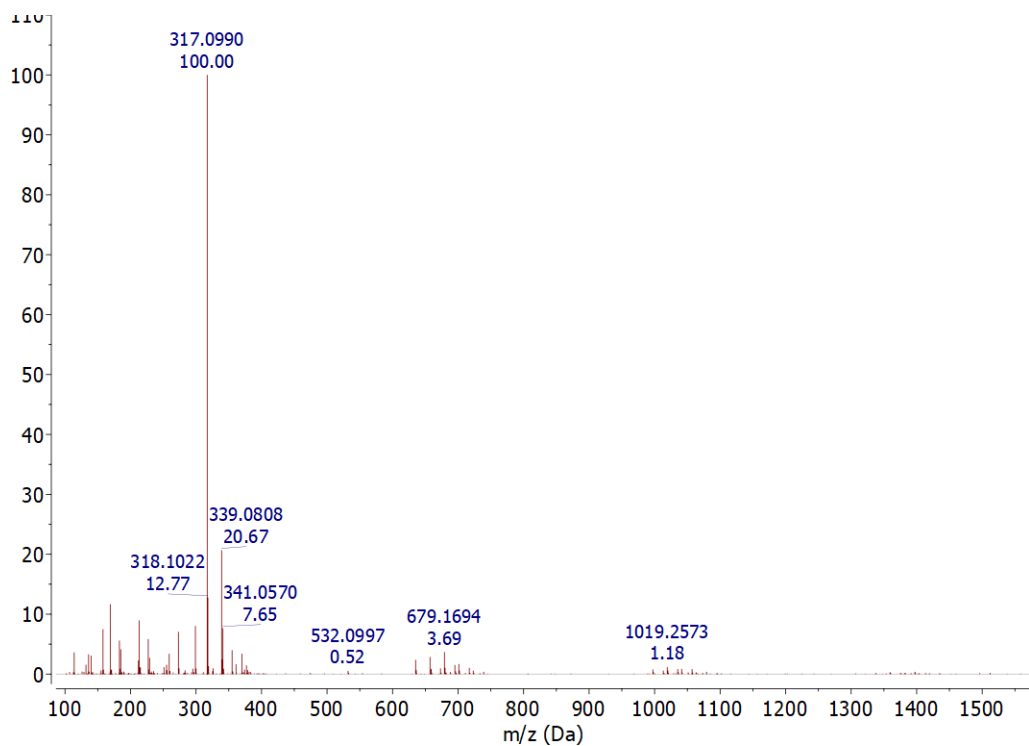


Figure S12. Experimental high resolution mass spectrum (ESI⁻) of **H₄L1**.

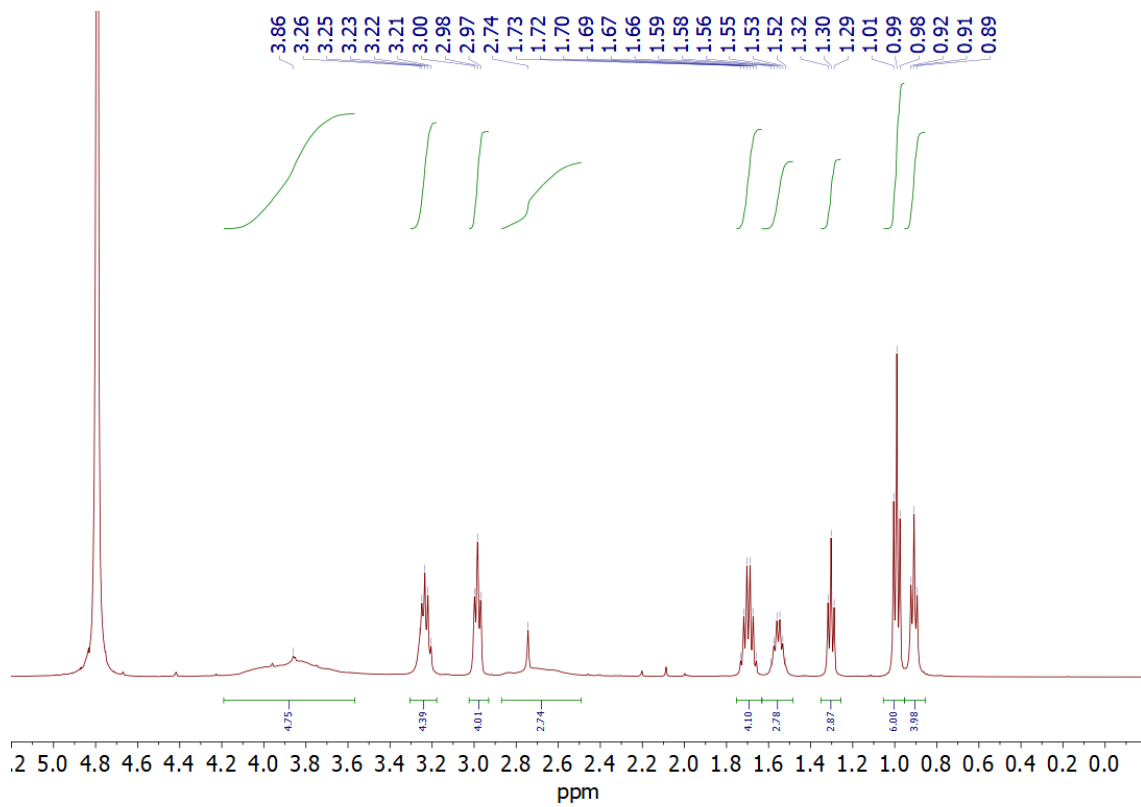


Figure S13. ¹H NMR spectrum of H₂L3 (500 MHz, D₂O, pH = 2.10, 298 K).

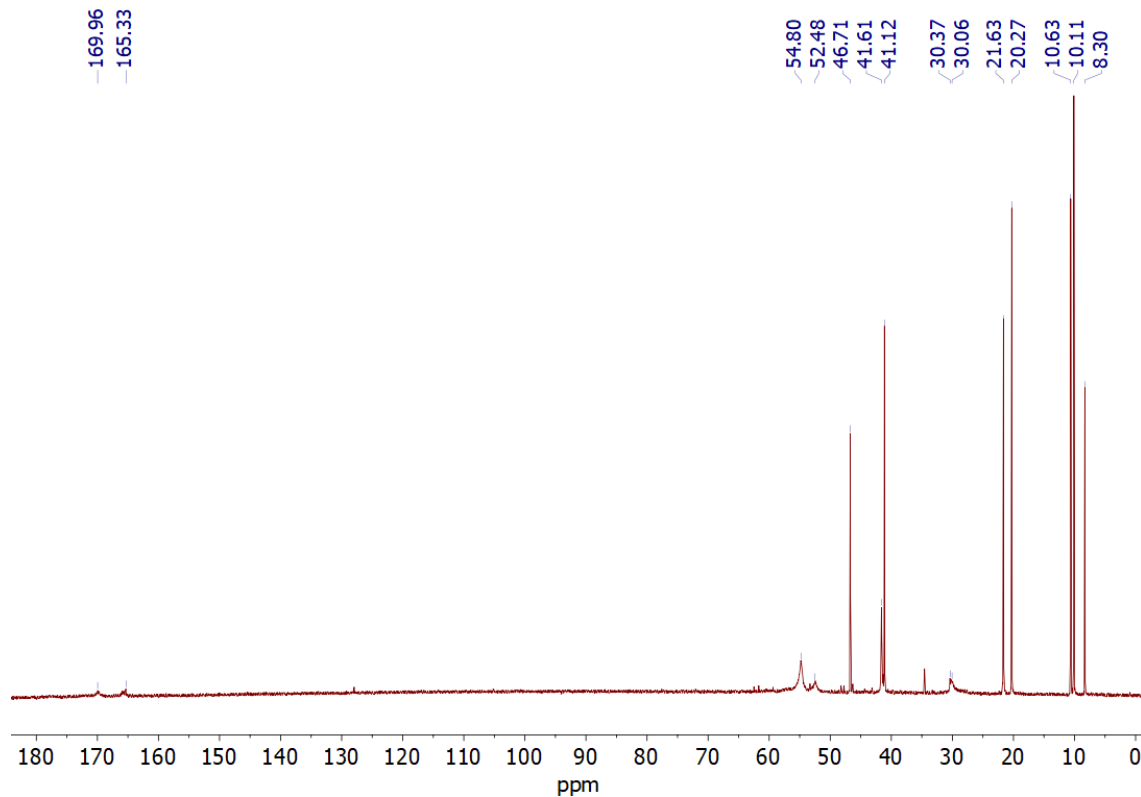


Figure S14. ¹³C NMR spectrum of H₂L3 (126 MHz, D₂O, pH = 2.10, 298 K).

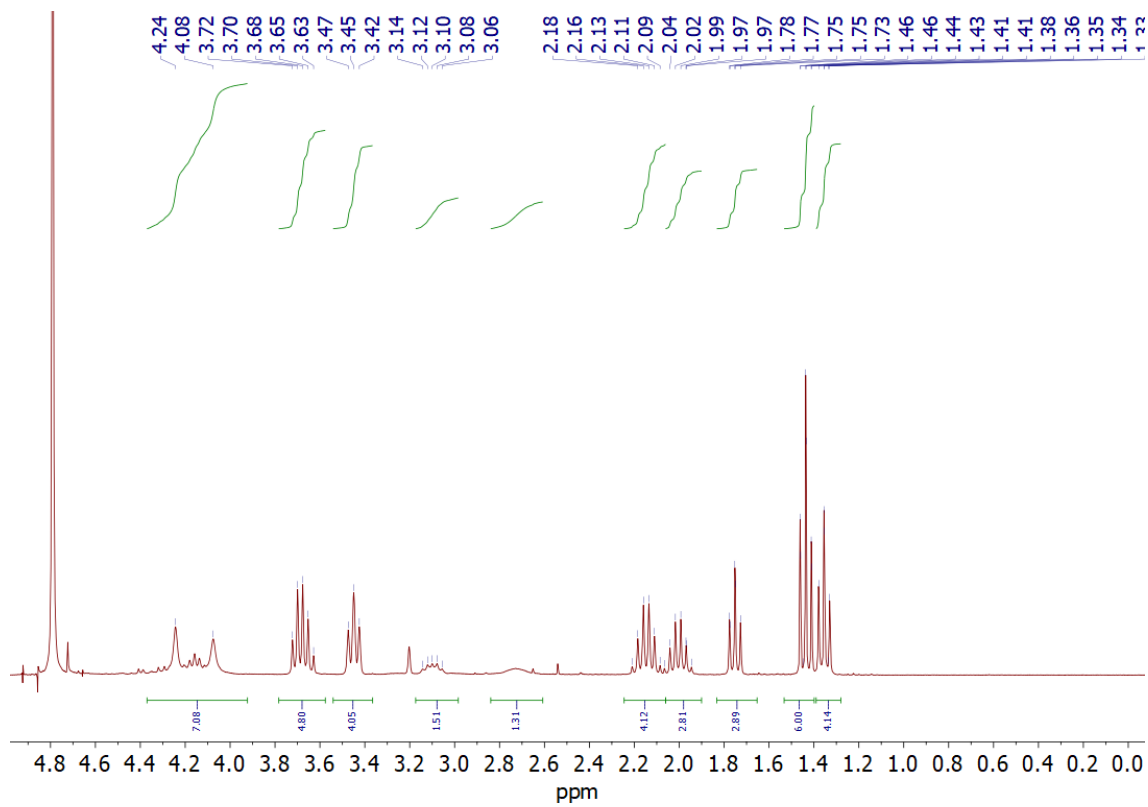


Figure S15. ¹H NMR spectrum of **H₂L3** (300 MHz, D₂O, pH = 2.10, 343 K).

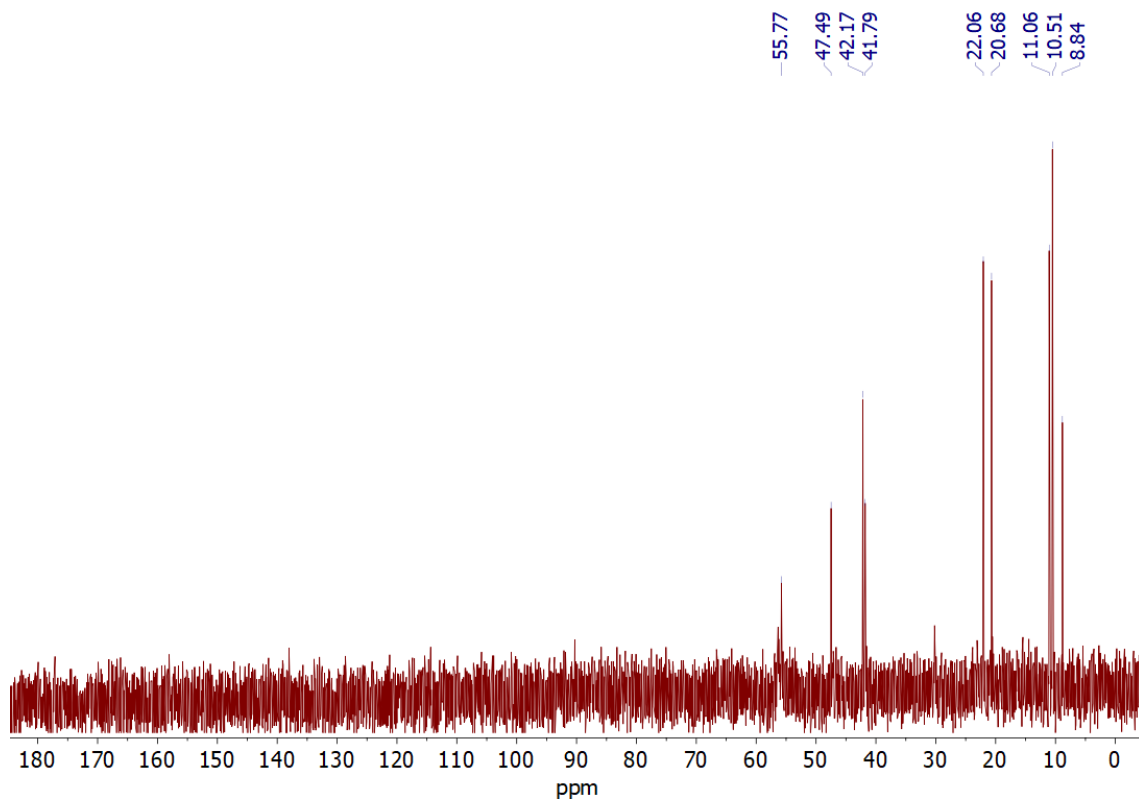


Figure S16. ¹³C NMR spectrum of **H₂L3** (75.5 MHz, D₂O, pH = 2.10, 343 K).

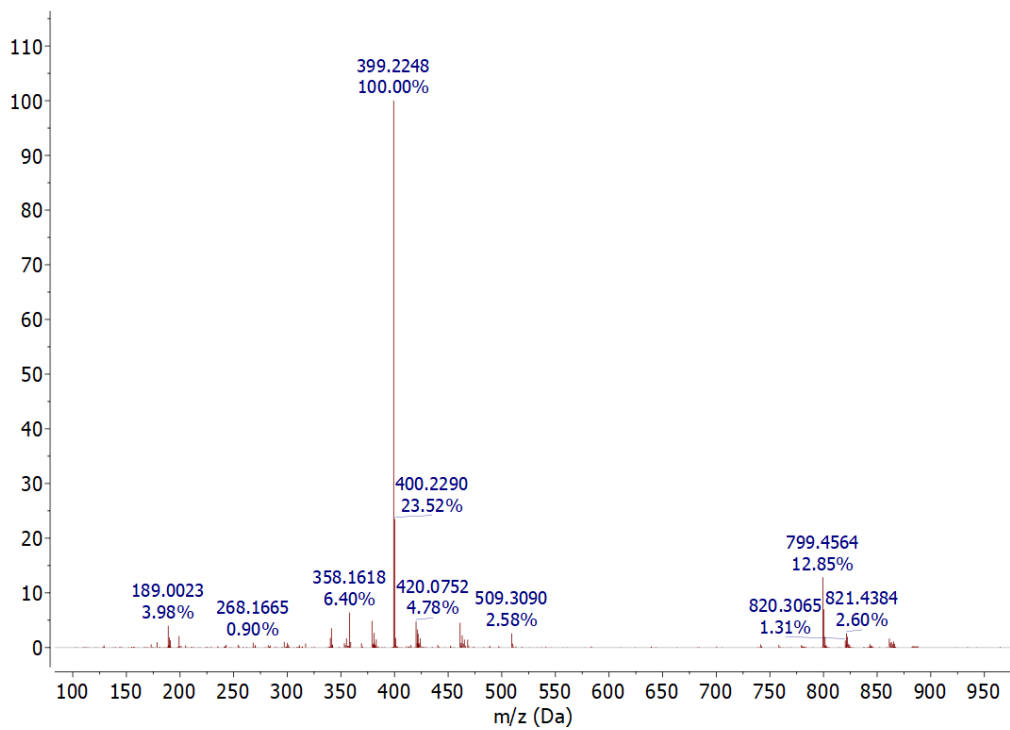


Figure S17. Experimental high resolution mass spectrum (ESI⁺) of H₂L3.

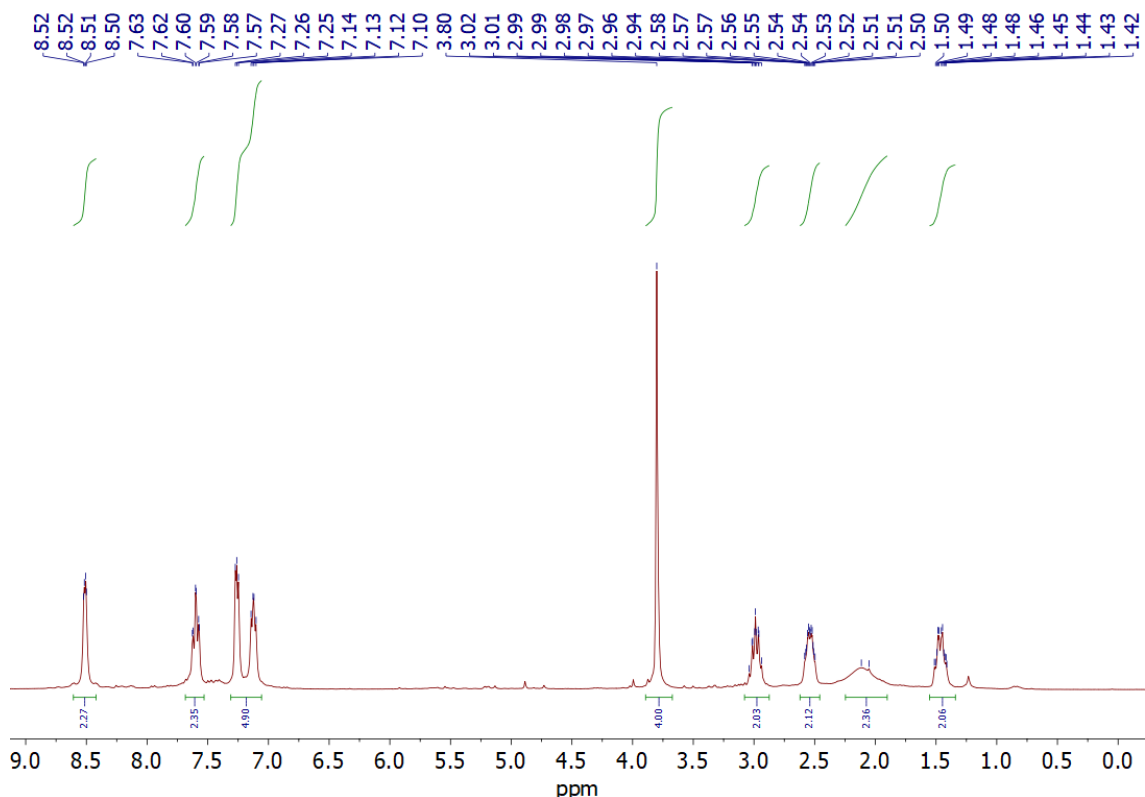


Figure S18. ^1H NMR spectrum of compound **2** (300 MHz, CDCl_3 , 298 K).

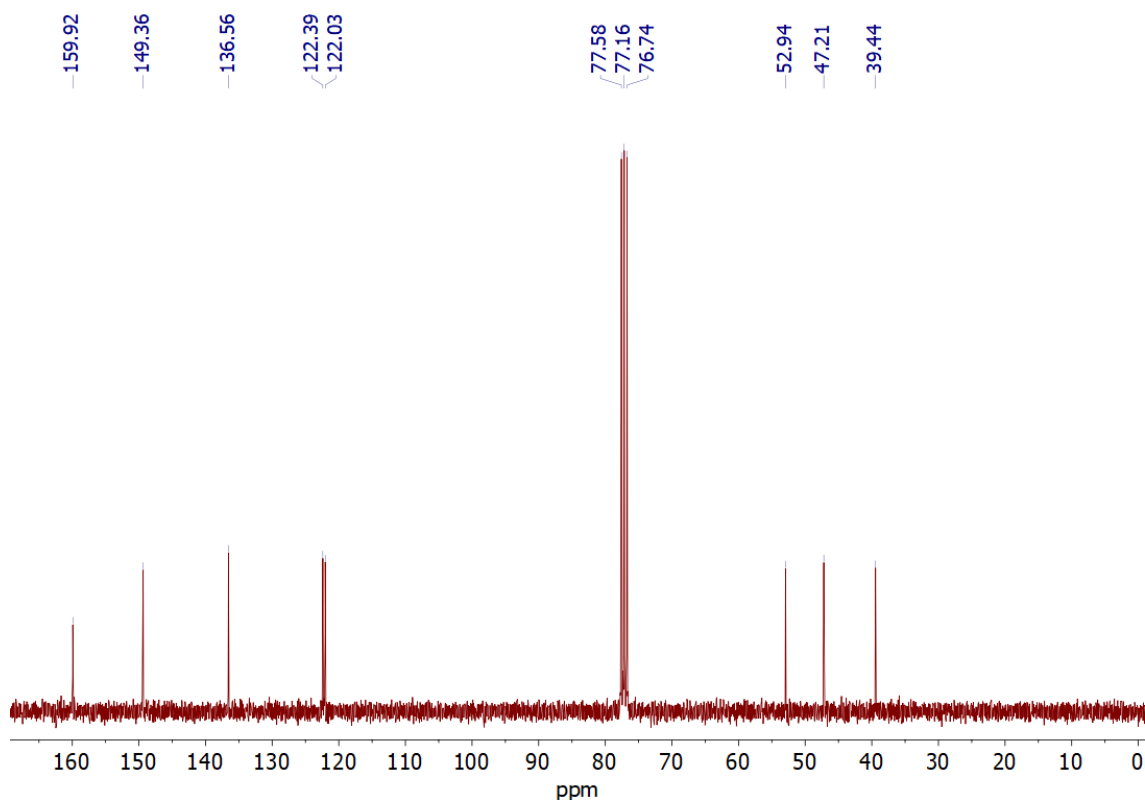


Figure S19. ^{13}C NMR spectrum of compound **2** (75.5 MHz, CDCl_3 , 298 K).

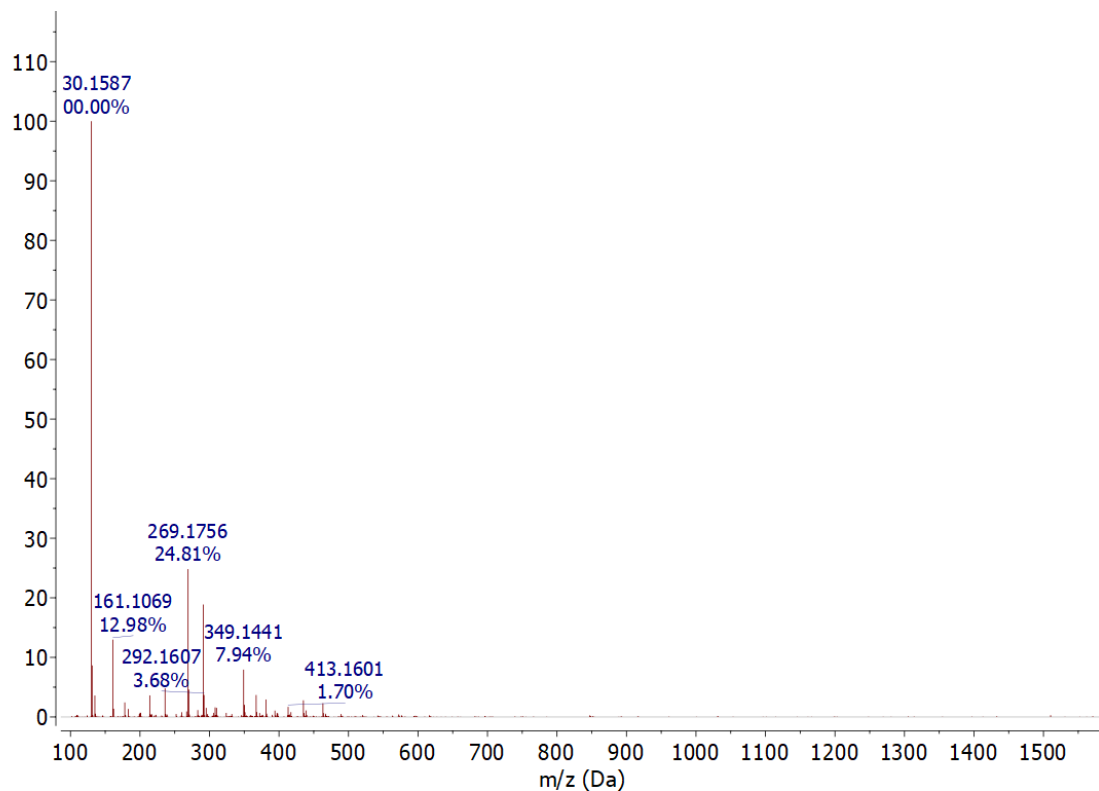


Figure S20. Experimental high resolution mass spectrum (ESI^+) of compound 2.

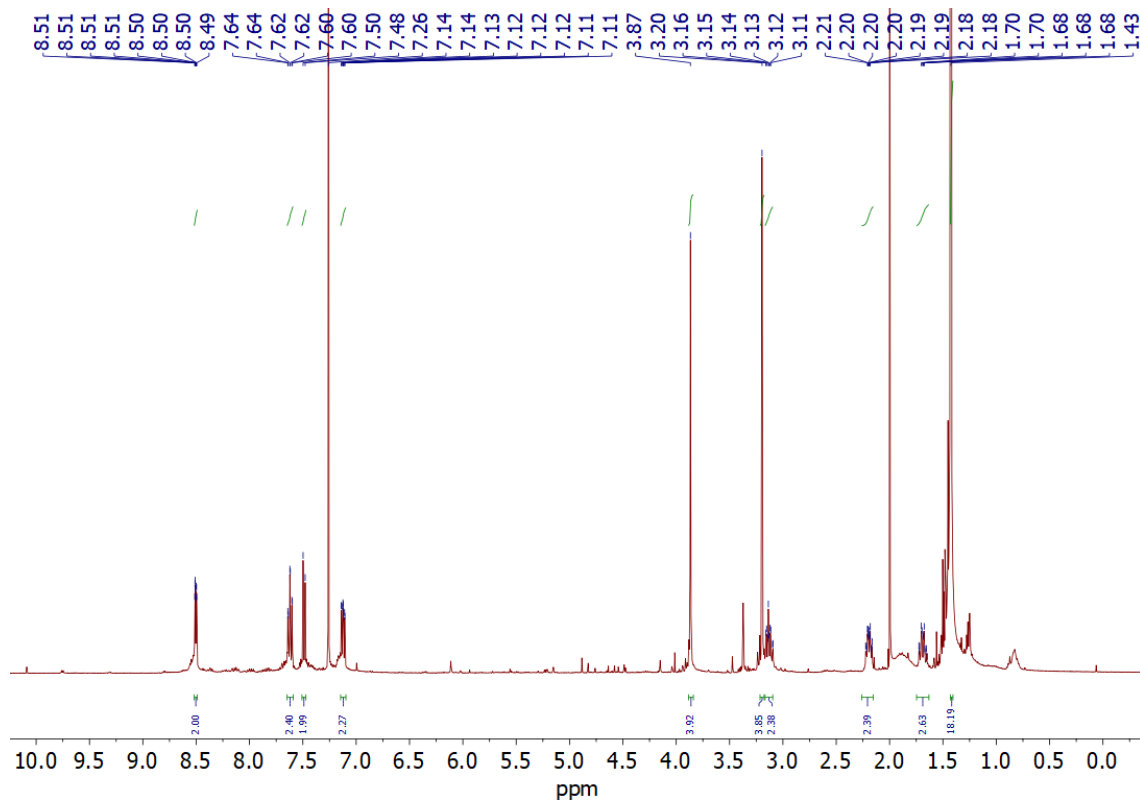


Figure S21. ^1H NMR spectrum of compound **3** (400 MHz, CDCl_3 , 298 K).

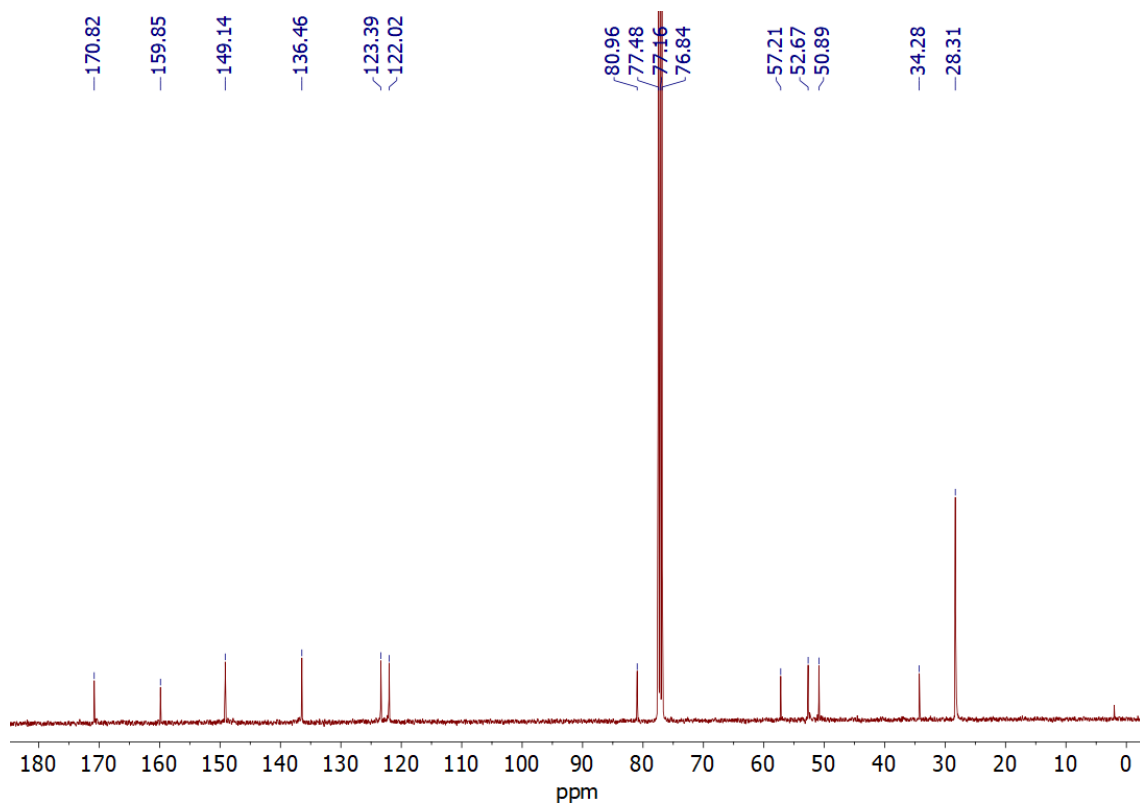


Figure S22. ^{13}C NMR spectrum of compound **3** (101 MHz, CDCl_3 , 298 K).

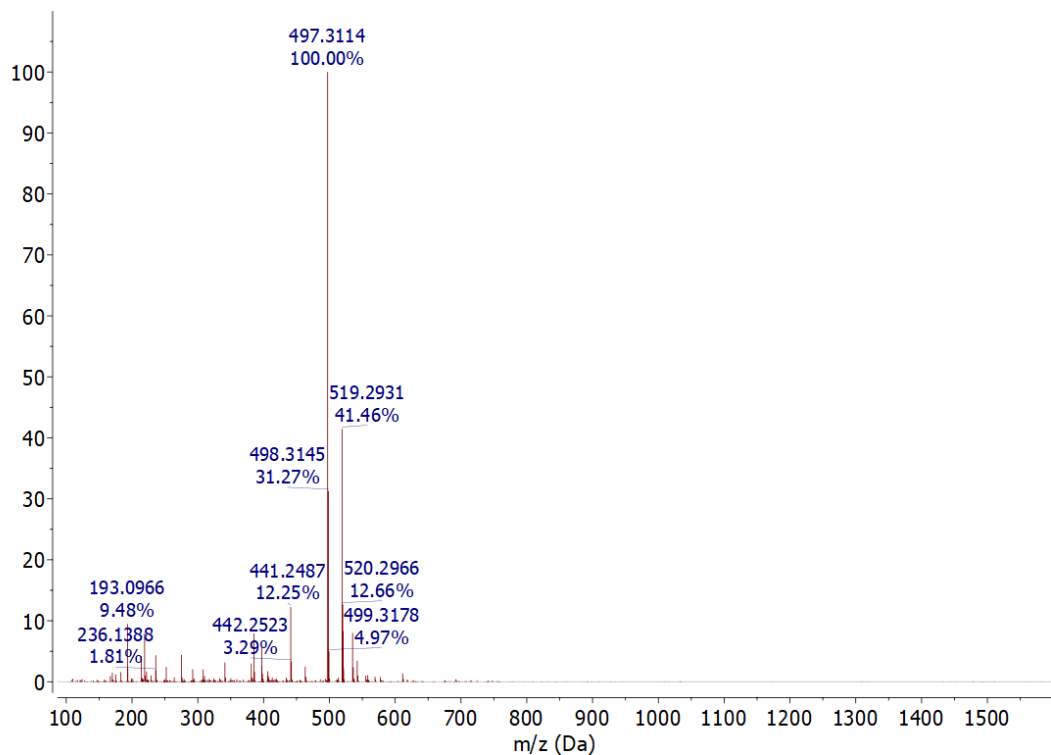


Figure S23. Experimental high resolution mass spectrum (ESI^+) of compound 3.

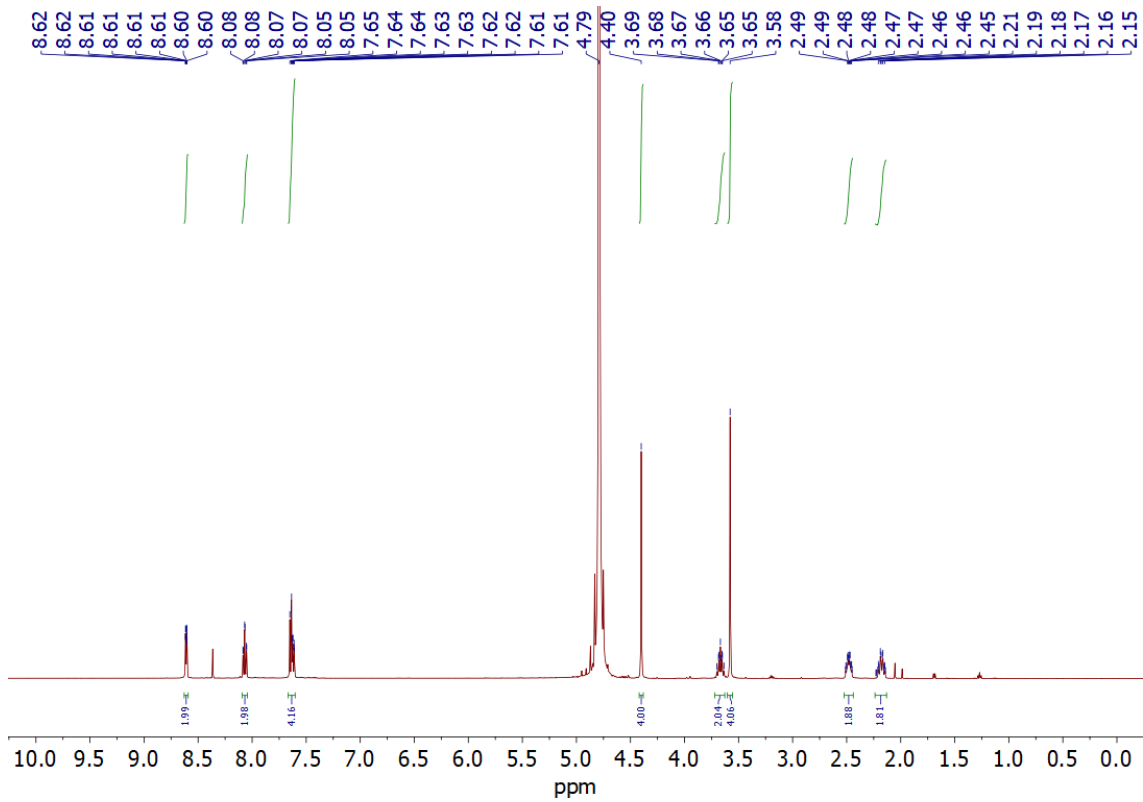


Figure S24. ^1H NMR spectrum of $\text{H}_2\text{L2}$ (500 MHz, D_2O , pH 4.33, 298 K).

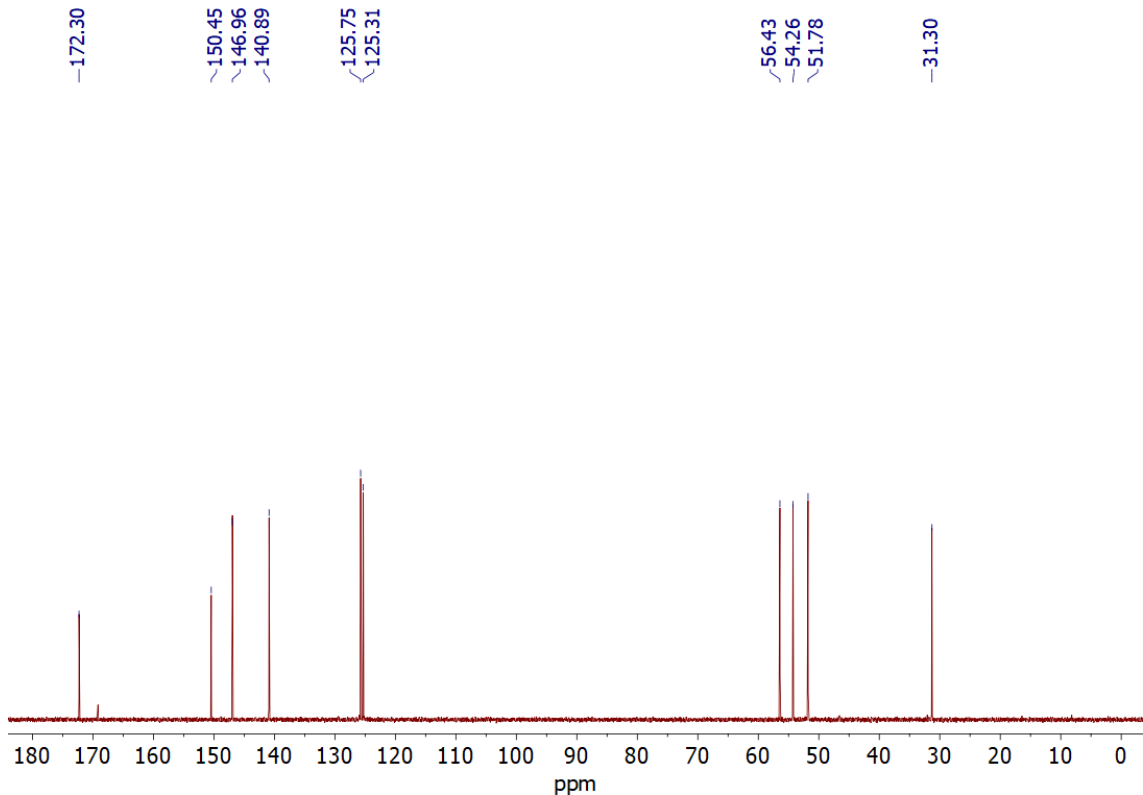


Figure S25. ^{13}C NMR spectrum of $\text{H}_2\text{L2}$ (126 MHz, D_2O , pH 4.33, 298 K).

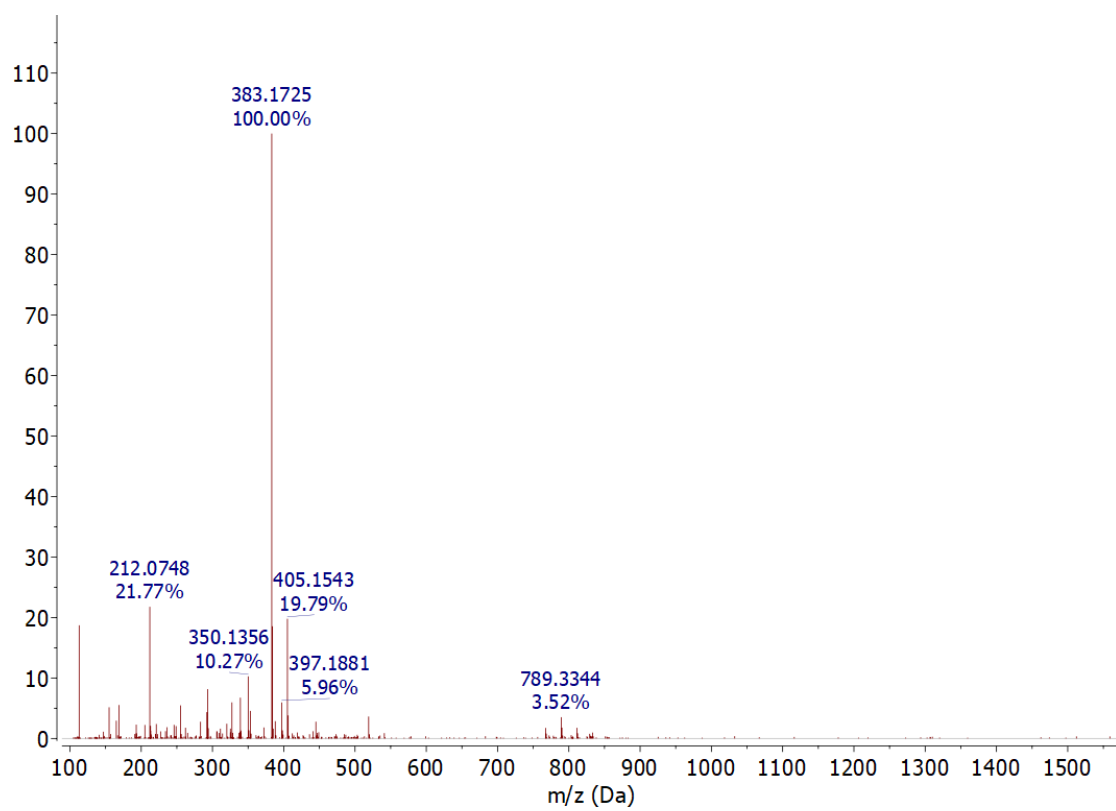


Figure S26. Experimental high resolution mass spectrum (ESI^+) of $\text{H}_2\text{L2}$.

Table S1. Optimized Cartesian coordinates obtained for $[\text{Mn}(\text{EDTA})(\text{H}_2\text{O})]^{2-}\cdot 5\text{H}_2\text{O}$ (M11/Def2-TZVPP, scrf=pcm).

Center Number	Atomic Number	Coordinates (Angstroms)		
		X	Y	Z
1	8	2.261552	-0.721128	1.366625
2	8	3.750417	-2.382156	1.260291
3	8	2.701827	3.027558	-1.478846
4	8	1.004032	1.892436	-0.575313
5	8	-0.271492	-2.128191	0.636871
6	8	-1.986805	-3.529899	0.378332
7	8	-1.692816	1.014165	0.145010
8	8	-2.735047	2.265054	-1.378289
9	7	-0.825286	-0.766197	-1.630219
10	7	2.059633	-0.496606	-1.281584
11	6	0.130306	-1.424389	-2.523239
12	1	0.307937	-2.429204	-2.122554
13	6	1.447073	-0.666505	-2.601325
14	1	1.272186	0.334416	-3.012327
15	6	2.714200	-1.691634	-0.769513
16	1	2.066552	-2.560406	-0.932371
17	1	3.676891	-1.891989	-1.263209
18	6	2.944708	-1.603146	0.748077
19	6	2.937936	0.667941	-1.258319
20	1	3.592876	0.605968	-0.382152
21	1	3.577375	0.724281	-2.150713
22	6	2.158356	1.984288	-1.111716
23	6	-1.823014	-1.706192	-1.137159
24	1	-2.700047	-1.155887	-0.778487
25	1	-2.171675	-2.393118	-1.922380
26	6	-1.313942	-2.531843	0.054628
27	6	-1.424692	0.445541	-2.165613
28	1	-0.658609	1.053647	-2.657477
29	1	-2.215883	0.242340	-2.902996
30	6	-2.005078	1.314762	-1.042782
31	8	0.078029	0.976752	2.364094
32	1	0.814200	0.891704	2.998369
33	1	-0.080157	1.926290	2.169650
34	8	-0.176083	3.518449	1.339225
35	8	2.350885	0.298522	3.823724
36	1	0.196262	3.097478	0.539095
37	1	-1.116903	3.699795	1.151311
38	1	2.259978	-0.327676	4.545952
39	1	2.464222	-0.219287	2.991011
40	25	0.349857	-0.025432	0.356829
41	8	-3.320702	-0.446996	1.958325
42	1	-2.778018	0.074732	1.344189
43	1	-3.787519	-1.123495	1.441748
44	8	-4.544749	-2.659550	0.602988
45	8	-2.886507	3.942854	0.741727
46	1	-2.912637	3.324878	-0.029374
47	1	-3.163619	4.805744	0.424201
48	1	-5.038675	-2.637864	-0.220202
49	1	-3.690788	-3.112296	0.425163
50	1	-0.286421	-1.549908	-3.535185
51	1	2.130157	-1.180626	-3.295716

E (UM11) ==-2709.8497385 Hartree

Zero-point correction=	0.387377
Thermal correction to Energy=	0.422871
Thermal correction to Enthalpy=	0.423815
Thermal correction to Gibbs Free Energy=	0.318406
Sum of electronic and zero-point Energies=	-2709.462361
Sum of electronic and thermal Energies=	-2709.426867
Sum of electronic and thermal Enthalpies=	-2709.425923
Sum of electronic and thermal Free Energies=	-2709.531333

Table S2. Optimized Cartesian coordinates obtained for $[\text{Mn}(\text{L1})(\text{H}_2\text{O})]^{2-}\cdot 5\text{H}_2\text{O}$ (M11/Def2-TZVPP, scrf=pcm).

Center Number	Atomic Number	Coordinates (Angstroms)		
		X	Y	Z
1	8	2.122059	0.345133	1.722947
2	8	3.890679	-0.751677	2.525078
3	8	2.593410	2.323780	-2.459712
4	8	0.935342	1.591560	-1.161243
5	8	-0.297858	-1.577165	1.421157
6	8	-1.876074	-3.130765	1.645132
7	8	-1.812036	0.996554	-0.105930
8	8	-3.155839	1.526241	-1.804123
9	7	-0.884104	-1.217005	-1.296804
10	7	2.274956	-0.826038	-0.685456
11	6	3.019758	-1.430459	0.417030
12	1	2.535849	-2.369840	0.704482
13	1	4.056925	-1.663208	0.135921
14	6	3.032401	-0.544825	1.664222
15	6	2.989071	0.338771	-1.222901
16	1	3.632624	0.755940	-0.441182
17	1	3.640544	0.057719	-2.060454
18	6	2.103420	1.513604	-1.671311
19	6	-1.764559	-2.018014	-0.440324
20	1	-2.724760	-1.503554	-0.318387
21	1	-1.988469	-2.992282	-0.895311
22	6	-1.261551	-2.267697	0.990151
23	6	-1.658620	-0.286531	-2.111219
24	1	-1.002567	0.194000	-2.842617
25	1	-2.463179	-0.788692	-2.668126
26	6	-2.265421	0.835559	-1.273736
27	8	-0.235731	1.865323	1.924236
28	1	0.460532	2.119331	2.550736
29	1	-0.421566	2.632437	1.348366
30	8	-0.433949	3.800475	-0.063719
31	8	2.005875	2.200397	3.629954
32	1	-0.036042	3.114201	-0.626236
33	1	-1.384151	3.837281	-0.273340
34	1	1.931069	1.852637	4.519970
35	1	2.206037	1.439399	3.035977
36	25	0.294441	0.218254	0.388705
37	8	-3.468715	0.164837	2.054448
38	1	-2.892169	0.464267	1.334883
39	1	-3.861338	-0.677403	1.783724
40	8	-4.507395	-2.471346	1.522972
41	8	-3.207922	3.879922	-0.498695
42	1	-3.277041	3.009809	-0.958910
43	1	-3.565908	4.540457	-1.093879
44	1	-4.963196	-2.784678	0.740179
45	1	-3.615030	-2.875781	1.522152
46	6	2.049787	-1.824353	-1.737165
47	6	-0.063004	-2.081286	-2.151523
48	6	0.989701	-2.880413	-1.352627
49	6	1.094556	-1.328317	-2.841825
50	1	0.989368	-0.249540	-2.957489
51	1	1.336809	-1.774271	-3.807650
52	1	0.795747	-3.017801	-0.288472

53	1	1.199330	-3.845086	-1.817107
54	1	-0.709266	-2.674702	-2.814251
55	1	3.014858	-2.218085	-2.087428

E (UM11) = -2787.2538319 Hartree
 Zero-point correction= 0.422863
 Thermal correction to Energy= 0.459836
 Thermal correction to Enthalpy= 0.460781
 Thermal correction to Gibbs Free Energy= 0.353138
 Sum of electronic and zero-point Energies= -2786.830968
 Sum of electronic and thermal Energies= -2786.793995
 Sum of electronic and thermal Enthalpies= -2786.793051
 Sum of electronic and thermal Free Energies= -2786.900694

Table S3. Optimized Cartesian coordinates obtained for [Mn(**L2**)(H₂O)]·2H₂O (M11/Def2-TZVPP, scrf=pcm).

Center Number	Atomic Number	Coordinates (Angstroms)		
		X	Y	Z
1	8	-1.414509	-1.210616	-3.604071
2	8	0.049343	-0.880019	-1.959427
3	8	-0.168795	0.913961	1.889221
4	8	0.771472	2.172841	3.471279
5	7	1.788670	1.597752	0.045042
6	7	-1.270948	1.451100	-1.106282
7	6	-2.436981	1.632986	-0.237180
8	1	-2.111095	2.114977	0.689518
9	1	-3.183229	2.288605	-0.711653
10	6	-1.641821	0.797434	-2.376195
11	1	-2.720580	0.625259	-2.428251
12	1	-1.395801	1.452849	-3.219808
13	6	-0.961524	-0.547326	-2.673578
14	6	2.016680	1.817384	1.480120
15	1	2.733613	1.071302	1.841814
16	1	2.451644	2.807143	1.670063
17	6	0.772075	1.642946	2.363836
18	6	3.018236	1.138430	-0.606731
19	1	2.867468	1.179058	-1.691063
20	1	3.858156	1.810117	-0.374787
21	8	-0.038389	-2.008104	1.481084
22	1	-0.756685	-1.843855	2.119018
23	1	-0.259123	-2.758118	0.909401
24	8	-0.257258	-3.411802	-0.909441
25	8	-1.825304	-0.795641	3.215023
26	1	-0.083392	-2.634150	-1.474640
27	1	0.212810	-4.157272	-1.286548
28	1	-1.311487	-0.029506	2.887923
29	1	-1.712656	-0.824586	4.166841
30	25	0.151648	-0.199027	0.065316
31	6	-0.652194	2.757199	-1.377707
32	6	1.375495	2.846222	-0.618375
33	6	0.017429	3.402168	-0.147758
34	6	0.746755	2.594521	-2.008229
35	1	0.945285	1.620117	-2.463281
36	1	0.981765	3.389152	-2.717233
37	1	-0.342320	3.113259	0.837630
38	1	0.002101	4.490080	-0.227732
39	1	2.208641	3.561819	-0.588208
40	1	-1.358353	3.397959	-1.923014
41	6	-3.090091	0.320304	0.112834
42	6	-4.435658	0.277386	0.457632
43	6	-5.014162	-0.943227	0.746524
44	1	-5.014329	1.195705	0.482748
45	6	-2.905249	-1.954085	0.319129
46	6	-4.236926	-2.088485	0.659761
47	1	-6.063942	-1.004598	1.018325
48	1	-2.269147	-2.830067	0.224815
49	1	-4.653243	-3.071427	0.851163
50	6	3.389430	-0.276320	-0.244771
51	6	4.716868	-0.679686	-0.294868
52	6	5.027896	-1.998730	-0.025420

53	1	5.488459	0.042247	-0.543637
54	6	2.710103	-2.385392	0.343420
55	6	4.002322	-2.872805	0.297406
56	1	6.058214	-2.340350	-0.060926
57	1	1.884190	-3.035754	0.607445
58	1	4.196159	-3.916297	0.519945
59	7	-2.334350	-0.773881	0.065569
60	7	2.403928	-1.113324	0.076071

E(UM11) =-2675.6549597 Hartree
 Zero-point correction= 0.483341
 Thermal correction to Energy= 0.516321
 Thermal correction to Enthalpy= 0.517266
 Thermal correction to Gibbs Free Energy= 0.418109
 Sum of electronic and zero-point Energies= -2675.171619
 Sum of electronic and thermal Energies= -2675.138638
 Sum of electronic and thermal Enthalpies= -2675.137694
 Sum of electronic and thermal Free Energies= -2675.236850

Table S4. Optimized Cartesian coordinates obtained for [Mn(**L3**)(H₂O)]·2H₂O (M11/Def2-TZVPP, scrf=pcm).

Center Number	Atomic Number	Coordinates (Angstroms)		
		X	Y	Z
1	8	-2.310244	0.748621	-0.644473
2	8	-0.258209	1.642506	3.529054
3	8	0.453754	1.142015	1.476107
4	8	-0.373493	-1.253083	-1.904983
5	8	0.431493	-2.963931	-3.086719
6	8	2.121413	0.822568	-1.080476
7	7	1.598981	-1.559300	0.037775
8	7	-1.344433	-0.945287	1.247362
9	6	-2.600939	-1.287852	0.594850
10	1	-2.436905	-2.134527	-0.081131
11	1	-3.380589	-1.579498	1.315900
12	6	-3.094715	-0.139387	-0.261025
13	6	-1.538561	0.077569	2.283951
14	1	-2.380764	0.722361	2.007395
15	1	-1.781938	-0.375107	3.254653
16	6	-0.346643	1.029533	2.468349
17	6	1.757012	-2.181736	-1.284029
18	1	2.524056	-1.643839	-1.851651
19	1	2.091450	-3.224112	-1.195895
20	6	0.496658	-2.145577	-2.167187
21	6	2.814937	-0.877838	0.459110
22	1	2.701354	-0.540031	1.495012
23	1	3.701120	-1.530659	0.412861
24	6	3.038705	0.362178	-0.389702
25	8	-0.025574	2.459566	-1.206646
26	1	-0.828269	3.008401	-1.150986
27	1	0.699521	2.908742	-0.735619
28	8	1.748636	3.411708	0.760811
29	8	-2.601860	3.464308	-1.099011
30	1	1.395639	2.600129	1.187599
31	1	2.704967	3.391530	0.846077
32	1	-3.013460	3.765707	-1.913395
33	1	-2.743635	2.503101	-1.034462
34	25	-0.024082	0.283106	-0.469312
35	6	-0.757826	-2.161031	1.835662
36	6	1.214761	-2.569545	1.032928
37	6	-0.196991	-3.144112	0.786362
38	6	0.684470	-1.965152	2.349676
39	1	1.002685	-0.955002	2.605676
40	1	0.886282	-2.630835	3.191256
41	1	-0.595742	-3.081144	-0.226514
42	1	-0.268433	-4.174478	1.140177
43	1	2.018822	-3.313477	1.134736
44	1	-1.463500	-2.587395	2.563853
45	7	-4.372762	-0.141473	-0.589604
46	7	4.242290	0.917416	-0.330654
47	1	-4.965144	-0.866587	-0.213732
48	1	4.951878	0.459339	0.221449
49	6	-4.954586	0.866414	-1.461417
50	1	-5.931091	0.518468	-1.797087
51	1	-5.075230	1.816009	-0.930148
52	1	-4.307001	1.016608	-2.329340

53	6	4.598973	2.117777	-1.068600
54	1	5.172753	1.867818	-1.966063
55	1	3.679281	2.625759	-1.362839
56	1	5.196572	2.773912	-0.432036

E(UM11) ==	-2597.5663425 Hartree
Zero-point correction=	0.454371
Thermal correction to Energy=	0.487784
Thermal correction to Enthalpy=	0.488728
Thermal correction to Gibbs Free Energy=	0.388868
Sum of electronic and zero-point Energies=	-2597.111972
Sum of electronic and thermal Energies=	-2597.078559
Sum of electronic and thermal Enthalpies=	-2597.077615
Sum of electronic and thermal Free Energies=	-2597.177474

References

1 F. K. Kálmán and G. Tircsó, *Inorg. Chem.*, 2012, **51**, 10065–10067.